

# An improved neighborhood algorithm: Parameter conditions and dynamic scaling

Marc Wathelet

► **To cite this version:**

Marc Wathelet. An improved neighborhood algorithm: Parameter conditions and dynamic scaling. *Geophysical Research Letters*, American Geophysical Union, 2008, 35 (9), pp.NIL\_26-NIL\_30. 10.1029/2008GL033256 . insu-00335912

**HAL Id: insu-00335912**

**<https://hal-insu.archives-ouvertes.fr/insu-00335912>**

Submitted on 11 Mar 2021

**HAL** is a multi-disciplinary open access archive for the deposit and dissemination of scientific research documents, whether they are published or not. The documents may come from teaching and research institutions in France or abroad, or from public or private research centers.

L'archive ouverte pluridisciplinaire **HAL**, est destinée au dépôt et à la diffusion de documents scientifiques de niveau recherche, publiés ou non, émanant des établissements d'enseignement et de recherche français ou étrangers, des laboratoires publics ou privés.

# An improved neighborhood algorithm: Parameter conditions and dynamic scaling

M. Wathelet<sup>1</sup>

Received 18 January 2008; revised 24 March 2008; accepted 28 March 2008; published 3 May 2008.

[1] The Neighborhood Algorithm (NA) is a popular direct search inversion technique. For dispersion curve inversion, physical conditions between parameters  $V_s$  and  $V_p$  (linked by Poisson's ratio) may limit the parameter space with complex boundaries. Other conditions may come from prior information about the geological structure. Irregular limits are not natively handled by classical search algorithms. In this paper, we extend the NA formulation to such parameter spaces. For problems affected by non-uniqueness, the ideal solution is made of the ensemble of all models that equally fits the data and prior information. Hence, a powerful exploration tool is required. Exploiting the properties of the Voronoi cells, we show that a dynamic scaling of the parameters during the convergence to the solutions drastically improves the exploration. **Citation:** Wathelet, M. (2008), An improved neighborhood algorithm: Parameter conditions and dynamic scaling, *Geophys. Res. Lett.*, 35, L09301, doi:10.1029/2008GL033256.

## 1. Introduction

[2] Inversion techniques are widespread in geophysics as attested by the number of scientific activities dealing with their development and their application, mostly since the beginning of the computer era. Inversion tools include linearized methods [Nolet, 1981; Tarantola, 1987] and direct search techniques [Sen and Stoffa, 1991; Lomax and Snieder, 1994] that gained success during the nineties parallel to the development of the power of desk computers. For inversion problems with a reduced number of unknowns, direct search methods are probably best suited because of their ability to correctly map the uncertainties of the problem in the case of non-uniqueness (distinct equivalent solutions).

[3] The Neighborhood Algorithm (NA) [Sambridge, 1999] is a stochastic direct search method that belongs to the same family as Genetic Algorithms (GA) [Lomax and Snieder, 1994] or Simulated Annealing (SA) [Sen and Stoffa, 1991]. Compared to a basic Monte Carlo sampling, these approaches try to guide the random generation of samples by the results obtained so far on previous samples. The areas of the parameter space where no interesting solution can be found are less sampled than promising areas. All methods require several tuning parameters to control the balance between exploitation and exploration, i.e. between a quick convergence to a minimum of the misfit function and slow investigation of nearly all local minima to find the global one or identify equivalent minima.

[4] NA makes use of Voronoi cells to model the misfit function across the parameter space. The misfit function is supposed to be known for  $n_{s0}$  samples randomly distributed or not over the parameter space. A Voronoi cell centered around one of these samples is the nearest neighbor region defined under a suitable distance norm (usually Euclidean). The union of all cells with a low misfit is the area of interest where new samples with small misfits are expected. The size of this ensemble is defined by the tuning parameter  $n_r$  (number of best cells to consider). Sambridge [1999] proposed a simple but very efficient way to generate new random samples inside a Voronoi cell based on a Gibbs sampler.  $n_s$  (second tuning parameter) new samples are generated and added to the original population ( $n_s/n_r$  samples per cell are added). The geometry of the initial Voronoi cells are modified to include these new  $n_s$  samples. The process is repeated  $it_{max}$  (last tuning parameter) times until an acceptable sampling of the solution is obtained.

[5] We take the classical inversion of shear wave velocity profiles from surface wave dispersion curves as an example. We first show that a good parameterization requires a parameter space with irregular conditions whereas the original NA is limited to an hyper-box. A suitable modification of the NA kernel is proposed. Secondly, we improve the exploration capabilities of NA by playing on parameter scales. It is particularly useful for inversion problems affected by non-uniqueness.

## 2. Searching Inside Irregular Boundaries

[6] In tabular ground structures (made of homogeneous and horizontal layers), typically used for the computation of dispersion curves, four parameters can fully describe an elastic layer:  $V_s$ ,  $H$  (thickness),  $V_p$ , and  $\rho$  (density). They are given by decreasing influence, especially the density can be considered as constant.  $V_s$  and  $V_p$  are directly related through the Poisson's Ratio ( $\nu$ ) which generally ranges from 0.2 to 0.5 in the nature. Historically, the effect of  $V_p$  over the dispersion curve has been considered as negligible. Nevertheless, Wathelet [2005] showed that this is not true for all Poisson's ratio values, particularly for those encountered for hard rocks (below 0.3).

### 2.1. Parameters of a Layer: $V_p$ , $V_s$ , or $\nu$ ?

[7] The usual approach, designed for linearized methods, divides the tabular structure into homogeneous layers with fixed thicknesses. Inside each layer, two options are generally available [Herrmann, 1994]: fixing  $V_p$  or  $\nu$ .  $V_s$  is left as the unique free parameter in all cases.  $V_p$  profiles measured by refraction experiments have their own uncertainties as recently recalled by Ivanov *et al.* [2006], and fixing definitively  $V_p$  to some arbitrary value may artificially reduce the

<sup>1</sup>LGIT, IRD, CNRS, Université Joseph Fourier, Grenoble, France.

range of possible solutions. Thus *Wathelet et al.* [2004] introduced another parameterization with two free parameters per layer:  $V_p$  and the ratio  $V_s/V_p$ , that has the advantage to keep all parameters to physically acceptable ranges. However,  $V_s$  is the most important parameter for surface wave problems. Not having a direct control over this parameter during the inversion is penalizing in most situations. Furthermore, in the context of stochastic inversion schemes,  $V_s$  is obtained by a non-linear combination of two random variables with uniform distributions ( $V_p$  and  $V_s/V_p$ ). Hence, the prior distribution of  $V_s$  is not uniform. Though uniform distributions cannot be considered as the total absence of prior information about a parameter value [Edwards, 1992], it is certainly closer to our prior knowledge than any uncontrolled and non uniform distribution (i.e. that supports some particular values rather than others) introduced by this non-linear combination used for computing  $V_s$ . The optimum parameterization would be  $V_s$  and  $V_p$  as free parameters compatible with Poisson's ratio conditions.

## 2.2. Freeing Thicknesses

[8] With the increasing success of stochastic inversion methods, velocities and thicknesses are both set as free parameters [e.g., *Wathelet et al.*, 2004; *Picozzi et al.*, 2005], which greatly helps reducing the number of degrees of freedom [Schurbaum et al., 2003]. Nevertheless, in a stack of  $N$  layers, the depth of the half-space top is thus the sum of  $N$  random variables with a uniform distribution and a finite variance. Using the Central Limit Theorem, the prior distribution of the bottom of the  $N^{\text{th}}$  layer tends towards a Gaussian. Hence, considering a large number of layers leads to generate models sticking around a median depth and not exploring any other depths for the deeper layers. For instance, with four layers above a half-space, the top of the half-space has only 5% chance to lie out of 4 standard deviations (from 85 to 315 m if the total possible range is from 0 to 400 m, a reduction of 42.5%). A possible solution would be to set up depth rather than thickness parameters. To generate valid ground models, the depth parameters must have greater values for deeper layers than for shallow ones, requiring some additional conditions.

## 2.3. Low Velocity Zones (LVZ)

[9] Surface wave methods, especially for active source experiments, are usually appreciated because they can investigate soft layers covered by stiffer ones [e.g., *Ryden and Park*, 2004]. LVZs may induce problems in the forward computation of the dispersion curve at high frequency (relative to the model structure): crossing modes can be encountered. Quick and straightforward algorithms are usually not suitable. Hence, during the random generation of models, the dispersion curve may be impossible to compute for some particular  $V_s$  profiles with LVZs. It defines an irregular limit to the parameter space that we can only estimate by trial and error. Lack of precision defining this complex boundary may eventually shadow parts of the parameter space containing low misfit solutions. Another aspect of LVZs is that they can potentially increase the number of possible solutions and the non-uniqueness of the problem. If our prior knowledge about the geological structure does not justify the presence of any LVZ, it would

be interesting to generate random  $V_s$  profiles without LVZ, requiring a simple condition at each interface.

## 2.4. Implementation

[10] In the above discussion, reviewing three aspects of the parameterization of tabular ground structures clearly shows the need for an inversion algorithm confined in a parameter space with complex boundaries. We assume the parameter space bounded by an hyper-box (classical limits) and by irregular limits, due to physical conditions, numerical limitations or prior information (Figure 1). The misfit computation is possible only inside the intersection of these two ensembles. By contrast with the hyper-box, the irregular limits may have no explicit definition (e.g. failure of the dispersion curve computation in case of strong LVZs).

[11] At the beginning of each iteration, the original NA generates  $n_s$  new models inside  $n_r$  cells. The corresponding misfits are computed in a second step by a user-provided function returning a floating-point value (implementation of the forward problem). To correctly handle failures of the misfit computation, we propose a function which returns an additional boolean value (true if it is a valid model). The generation of models by the Gibbs sampler must be integrated with the computation of misfits.  $n_c = n_s/n_r$  new samples are produced for each cell of the active region (union of all best  $n_r$  cells). If  $n_c$  is not an integer, it is rounded down and the remaining models are randomly distributed on the active cells. For each cell (repeated  $n_c$  times), the Gibbs sampler is used to generate a model and its misfit is directly computed. In case of success, the model is accepted the same way as in the original algorithm. If not, the returned misfit is ignored (it can be 0) and another model is randomly generated inside the cell until success. The original rigid concept of iterations has also been modified in a recent parallelization of the NA core [Rickwood and Sambridge, 2006]. Our conditional solution could be also developed for the parallel algorithm.

[12] When the active region is close to one of the complex boundaries, Voronoi cells where new samples are generated can be cut by one of them and only a small percentage of their multi-dimensional volume may be included inside the valid region (e.g. cell  $l$  in Figure 1). Thus, there might be only very little chance to generate one good sample even after a lot of trials. A way of solving this problem is to count all accepted and rejected models per cell. If the proportion of rejected models exceed a threshold (e.g. 90%), the cell is thrown away from the active region and replaced by the cell with the best misfit currently outside the active region.

[13] When there are a lot of conditions to satisfy, this random generator is not very efficient. A lot of invalid models must be rejected before accepting just one. If an explicit definition of the conditions is available, the Gibbs sampler can be modified to always return a valid model. For each parameter we define a list of conditions. A condition is a C++ object (a data structure with dedicated functions) that links several parameters together (it can be as simple as  $p1 < p2$ ). It has a mandatory function that returns the admissible range for each of its parameters, keeping all others constant. We assume that at least one model has successfully passed all conditions (model A in Figure 1). According to the original NA, to stay within cell  $k$ , parameter  $i$  can take any value from  $x_j$  to  $x_l$ . To fulfill the complex conditions  $x_l$  is

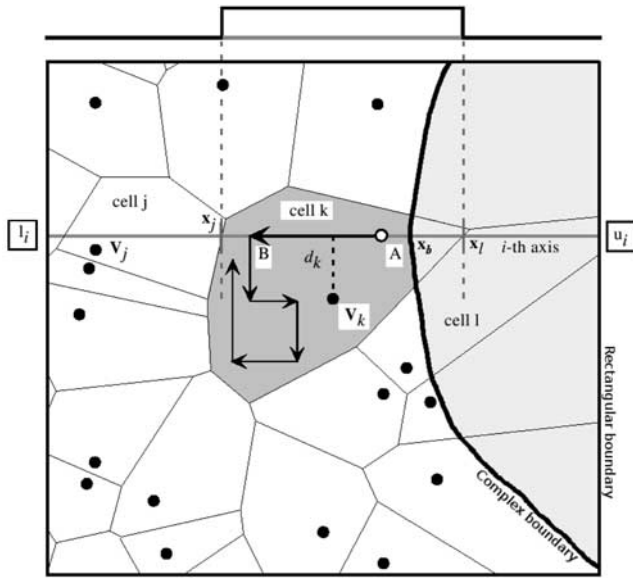


**Figure 1.** A uniform random walk restricted to a Voronoi cell and by complex boundaries (modified after *Sambridge* [1999, Figure 3]). Starting from a sample inside the cell ( $A$ ), a Markov-Chain random walk is achieved by introducing random perturbations along all axes successively. Each random perturbation (for instance along axis  $i$ ) is bounded by the rectangular boundary ( $l_i$  and  $u_i$ ), by the limits of the Voronoi cells ( $x_j$  and  $x_l$ ) and by the intersection of axis  $i$  passing by  $A$  with the complex boundary ( $x_b$ ). Asymptotically the samples produced by these walks are uniformly distributed inside the cell regardless of its shape [*Sambridge*, 1999]. The light grayed area is the region outside the parameter space still inside the rectangular boundary.

replaced by  $x_b$ ,  $x_b$  is computed exactly by the intersection of all admissible ranges given by all conditions available for parameter  $i$  keeping all other parameters constant. Hence, model  $A$  can be perturbed along axis  $i$  and the obtained model  $B$  is also satisfying all conditions. It is correct even if the admissible region is not convex. The process is repeated for all axes as in the original algorithm.

[14] Contrary to the original NA, even the initial population of samples ( $n_{s0}$ ) is generated by a Markov-Chain random walk based on a first valid model. The latter is obtained after a few iterations with an approximate definition of the complex boundary (because the current model is still outside the valid region).

[15] Thanks to this generic definition of conditions, we were able to introduce a new flexible parameterization that decouples all profiles of a tabular ground structure:  $V_p$  and  $V_s$  are defined separately with any kind of velocity variation inside the layers (uniform, linear, or power law). Prior information on  $V_p$  profile from refraction experiments can be introduced without constraining the layering for  $V_s$  profile. Poisson's ratio can be kept to reasonable values and LVZs are under control.

### 3. Exploration Capabilities of Parameter Scales

[16] *Sambridge* [1999] showed that one of the striking features of the Neighborhood algorithm is its ability to adapt

the sampling density and the center of sampling when better data-fitting models are discovered. The NA can jump out of local minima thanks to the randomness of the process and it can quickly evolve to a better solution. These properties are only meaningful for difficult inversion problems where the misfit function has multiple minima (e.g. the dispersion curve inversion).

[17] The fast escape comes directly from the geometrical properties of the Voronoi cells as illustrated in Figure 2 a. For instance, we assume that at the end of  $n$  iterations the best sample is  $A$ , the dark gray cell defines the region of best interest ( $n_r = 1$ ). If point  $B$  (white dot) is a new sample drawn randomly inside the dark gray cell, the Voronoi geometry at iteration  $n + 1$ , associated with the total population (first 10 samples and the new one), is the one shown with the dotted lines in Figure 2 a. If the misfit in point  $B$  is better than the misfit in point  $A$ , the region of interest clearly extends beyond its previous limits.

[18] Based on distances between sample points, the Voronoi geometry is not invariant to axis scaling factors. In Figure 2 b, the sample points are plotted with a different scale for the horizontal axis (factor 10 compared to Figure 2 a). The cell limits calculated for this second configuration are mostly aligned parallel to  $X$  axis. In such a scaled space, an equivalent process to the one presented for Figure 2 a would generate point  $B'$  whose associated cell has a totally different shape than the one related to point  $B$ . Cell  $B$  covers 31% of the total  $Y$  range whereas cell  $B'$  covers only 8%. On the contrary, for  $X$  axis, cell  $B$  covers only 22% whereas cell  $B'$  covers 100%. Hence, cell  $B'$  can potentially explore all values of parameter  $X$  and has a strongly limited search interval for parameter  $Y$ . By contrast, cell  $B$  explores all parameters with approximately the same weight.

[19] The influence of scaling factors may also be estimated from the number of inter-connections between cells,

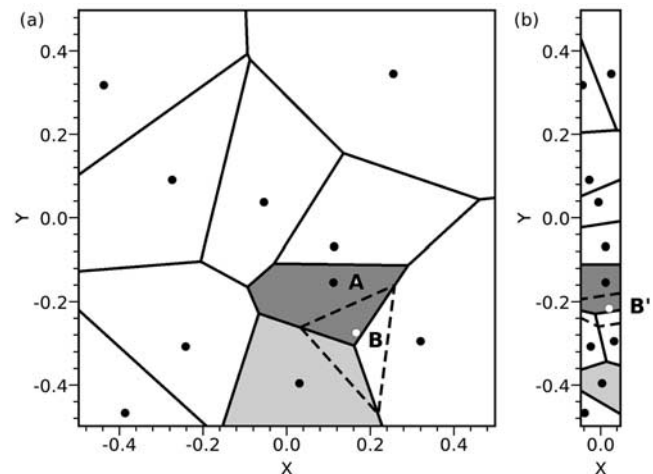


**Figure 2.** Effects of the axis scaling on cell connectivity for a 2D Voronoi geometry. (a) The two axes have the same scale (from  $-0.5$  to  $0.5$ ). The light gray and the dark gray cells are neighbors. (b)  $X$  axis is scaled by a factor 10 (from  $-0.05$  to  $0.05$ ). The two cells are not neighbors any longer. The dotted lines depict the modified Voronoi geometry after the addition of a point  $B$  (or  $B'$ ) at the limit of the cell centered around point  $A$ .

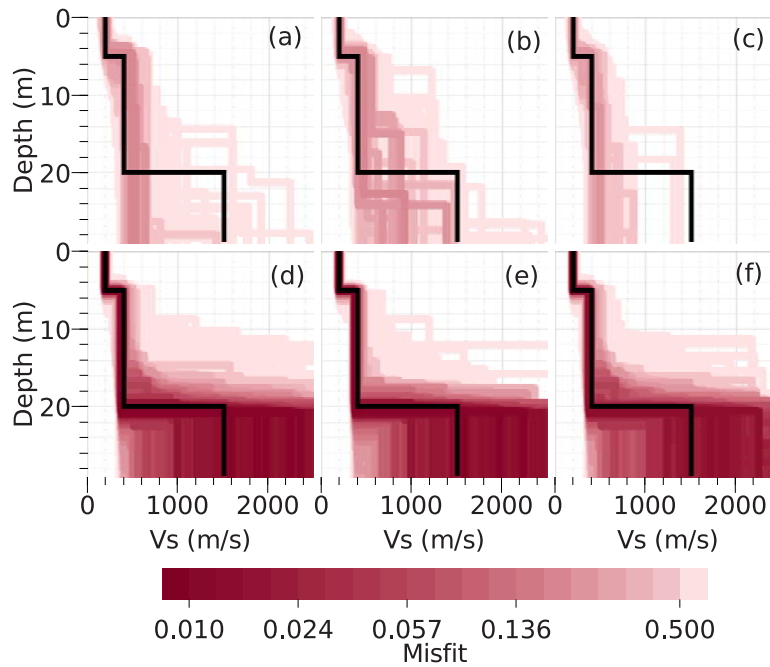


**Figure 3.** Effects of the parameter scaling on the search capabilities. The same high frequency dispersion curve (from 10 to 40 Hz) is inverted with the same parameterization (4 layers, 11 variable parameters). In all cases, 10050 samples are generated by a NA sampler (200 iterations with  $n_s$  and  $n_r$  set to 50). All  $V_s$  profiles with a misfit less than 1 are systematically shown. (a–c) The parameter space is scaled only at the beginning of the inversion process (static scaling, see text). (d–f) The parameter space is continuously scaled after each iteration (dynamic scaling, see text). Inside each group, three distinct seeds are randomly chosen to check the robustness of the results. The black curve is the true  $V_s$  profile.

which supports the exploration behavior of the NA. If we consider two neighbor samples (light and dark gray cells) in Figure 2 a, we observe that they are not neighbors in the same parameter space stretched along Y axis. In the second case, the region of interest cannot move towards lower Y values, blocked by previously generated samples with a higher misfit.

[20] If the parameter space contains parameters with strongly different sensibilities (e.g.  $V_s$  at different depths), the shape of the active region (union of all best  $n_r$  cells) may evolve during the inversion. Its size along well resolved axis is shortened and remains almost constant for poorly resolved parameters. From the results of Figure 2, as the number of iterations increases, this elongation leads to a better exploration of the already well resolved parameters. To the contrary, an efficient inversion process must be more exploratory for less resolved parameters. In the original NA, the parameters are eventually scaled to  $[0, 1]$  at the beginning of the inversion (called herein ‘static scaling’). By contrast, we propose a ‘dynamic scaling’ to maintain the exploration as constant as possible during the inversion. At the end of each NA iteration, the hyper-box surrounding the active region is computed. Each parameter is scaled by the size of the hyper-box along the corresponding axis. Scaling factors are tracked from the beginning to map scaled to real values and vice-versa.

[21] Figures 3a–3f compare the sampling achieved with static and dynamic scaling for the inversion of a realistic high frequency dispersion curve. The first 15 m of the ground structure are well recovered in all cases. In Figures 3a–3c, the inversion is clearly trapped in local

minima and the minimum achieved misfit is much higher (0.2) than for the dynamic scaling (Figures 3d and 3e, 0.01). In Figures 3d–3f, a loosely constrained parameter such as  $V_s$  in the deeper layers is much better investigated. Through the three distinct random seeds tested in Figure 3, the dynamic scaling results look quite robust: every inversion run gives almost the same picture compared to the static case. The maximum penetration depth of the method can be estimated with much more objectivity with a better exploration power. This example demonstrates one of the direct benefits of this improvement for surface wave practitioners.

#### 4. Conclusion

[22] We improved one of the popular direct search inversion techniques (Neighborhood Algorithm) originally well suited for investigating parameter spaces with simple rectangular limits. For practical inversion cases in geophysics, prior information about the geological settings or the geophysical parameters are to be included in the inversion to reduce the non-uniqueness of the problem. Furthermore, physical conditions may exist between parameters such as Poisson’s ratio linking  $V_p$  to  $V_s$ . To solve these questions, we developed a new algorithm capable of generating random samples inside a parameter space with irregular boundaries. In addition, we drastically improved the exploration behavior of the original algorithm through a dynamic scaling of parameter values. An efficient search of the parameter space ensures a convergence towards the global solution especially if sensibility is not equally distributed among parameters. Better uncertainty estimations are also naturally expected.

[23] Parameter conditions were mostly developed for the inversion of the dispersion curves of surface waves for 1D structures. It offers an easy way to introduce prior information in a fully controlled manner which may partly solve non-uniqueness. The range of applications is certainly not limited to the dispersion curve inversion. The non-uniqueness being present in a lot of other geophysical problems, we expect that this method might be of interest. The conditional technique developed here could also be adapted into Genetic Algorithms and Simulated Annealing codes.

[24] **Acknowledgments.** I would like to thank M. Sambridge for sharing his original code in Fortran (2002) and for his helpful review. Interesting comments from an anonymous reviewer also greatly improved the quality of the manuscript. I address my gratitude to Cecile Cornou, Pierre-Yves Bard and Denis Jongmans for reading preliminary versions of the manuscript. This work could be achieved thanks to the EU funding granted to the NERIES project (contract RII3-CT-2006-026130 of programme I3 - Integrated Infrastructure Initiative). The complete code described herein is available at <http://www.geopsy.org> under a GPL license.

## References

- Edwards, A. W. F. (1992), *Likelihood*, 2nd ed., John Hopkins Univ. Press, Baltimore, Md.
- Herrmann, R. B. (1994), *Computer Programs in Seismology*, vol. IV, St. Louis Univ., St. Louis, Mo.
- Ivanov, J., R. D. Miller, J. Xia, D. Steeples, and C. B. Park (2006), Joint analysis of refractions with surface waves: An inverse solution to the refraction-traveltime problem, *Geophysics*, 71, R131–R138.
- Lomax, A. J., and R. Snieder (1994), Finding sets of acceptable solutions with a genetic algorithm with application to surface wave group dispersion in Europe, *Geophys. Res. Lett.*, 21(24), 2617–2620.
- Nolet, G. (1981), Linearized inversion of (teleseismic) data, in *The Solution of the Inverse Problem in Geophysical Interpretation*, edited by R. Cassinis, pp. 9–37, Plenum, New York.
- Picozzi, M., S. Parolai, and S. M. Richwalski (2005), Joint inversion of H/V ratios and dispersion curves from seismic noise: Estimating the S-wave velocity of bedrock, *Geophys. Res. Lett.*, 32, L11308, doi:10.1029/2005GL022878.
- Rickwood, P., and M. Sambridge (2006), Efficient parallel inversion using the Neighbourhood Algorithm, *Geochem. Geophys. Geosyst.*, 7, Q11001, doi:10.1029/2006GC001246.
- Ryden, N., and C. B. Park (2004), Surface waves in inversely dispersive media, *Near Surf. Geophys.*, 2, 187–197.
- Sambridge, M. (1999), Geophysical inversion with a neighbourhood algorithm: I. Searching a parameter space, *Geophys. J. Int.*, 138, 479–494.
- Scherbaum, F., K.-G. Hinzen, and M. Ohrberger (2003), Determination of shallow shear wave velocity profiles in the Cologne/Germany area using ambient vibrations, *Geophys. J. Int.*, 152, 597–612.
- Sen, M. K., and P. L. Stoffa (1991), Nonlinear one-dimensional seismic waveform inversion using simulated annealing, *Geophysics*, 56, 1624–1638.
- Tarantola, A. (1987), *Inverse Problem Theory*, Elsevier, Amsterdam.
- Wathelet, M. (2005), Array recordings of ambient vibrations: surface-wave inversion. Ph.D. thesis, Univ. de Liège, Liège, Belgium.
- Wathelet, M., D. Jongmans, and M. Ohrberger (2004), Surface wave inversion using a direct search algorithm and its application to ambient vibration measurements, *Near Surf. Geophys.*, 2, 211–221.

---

M. Wathelet, LGIT, BP 53, F\_38041, Grenoble, Cedex 9, France.  
([marc.wathelet@ujf-grenoble.fr](mailto:marc.wathelet@ujf-grenoble.fr))